Received: 3 June 2019 | Accepted: 2 October 2019

DOI: 10.1113/EP087916

Experimental Physiology WILEY

RESEARCH PAPER

Breath-by-breath oxygen uptake during running: Effects of different calculation algorithms

Jessica Koschate[1] | Valentina Cettolo[2] | Uwe Hoffmann[1] | Maria Pia Francescato[2]

[1]Department of Medicine, University of Udine, Udine, Italy

[2]Institute of Exercise Training and Sport Informatics – Department of Exercise Physiology, German Sport University Cologne, Cologne, Germany

Correspondence
Maria Pia Francescato, Department of Medicine, University of Udine, P.le Kolbe 4, 33100, Udine, Italy.
Email: mariapia.francescato@uniud.it

Edited by: Michael White

Abstract

Recently, a new breath-by-breath gas exchange calculation algorithm (called 'independent breath') was proposed. In the present work, we aimed to compare the breath-by-breath O_2 uptake ($\dot{V}_{O_2}$) values assessed in healthy subjects undergoing a running protocol, as calculated applying the 'independent breath' algorithm or two other commonly used algorithms. The traces of respiratory flow, O_2 and CO_2 fractions, used by the calculation algorithms, were acquired at the mouth on 17 volunteers at rest, during running on a treadmill at 6.5 and 9.5 km h^{-1}, and thereafter up to volitional fatigue. Within-subject averages and standard deviations of breath-by-breath $\dot{V}_{O_2}$ were calculated for steady-state conditions; the $\dot{V}_{O_2}$ data of the incremental phase were analysed by means of linear regression, and their root mean square was assumed to be an index of the breath-by-breath fluctuations. The average values obtained with the different algorithms were significantly different ($P < 0.001$); nevertheless, from a practical point of view the difference could be considered 'small' in all the investigated conditions (effect size <0.3). The standard deviations were significantly lower for the 'independent breath' algorithm (*post hoc* contrasts, $P < 0.001$), and the slopes of the relationships with the corresponding data yielded by the other algorithms were <0.70. The root mean squares of the linear regressions calculated for the incremental phase were also significantly lower for the 'independent breath' algorithm, and the slopes of the regression lines with the corresponding values obtained with the other algorithms were <0.84. In conclusion, the 'independent breath' algorithm yielded the least breath-by-breath O_2 uptake fluctuation, both during steady-state exercise and during incremental running.

KEYWORDS

alveolar gas exchange, breath-by-breath fluctuations, dead space, gas exchange calculation algorithms, interchangeability

1 | INTRODUCTION

The assessment of breath-by-breath (BbB) gas exchange during exercise, namely, the measurement of O_2 uptake ($\dot{V}_{O_2}$; and/or CO_2 output) as occurs at the mouth, is a common procedure for sports medicine physicians and in scientific laboratories interested in exercise physiology. Although the information is acquired at the mouth, the gas exchange occurring at the alveolar-to-capillary membrane ('alveolar' gas exchange) can also be estimated, provided the BbB changes of lung gas stores are taken into account.

Recently, following the reasoning of Grønlund (1984), a new 'alveolar' gas exchange calculation algorithm has been proposed (called the 'independent breath' algorithm), which is based on an alternative view of the respiratory cycle (Cettolo & Francescato, 2015). In that view, the start and end points of the respiratory cycle are identified, during two consecutive expirations, as the times when equal ratios are observed between the O_2 fraction (or the CO_2 fraction) and the fraction obtained summing all other gases not exchanged at the alveolar-to-capillary membrane. Moreover, the algorithm allows the respiratory cycles to be partly superimposed or disjoined, neglecting

their contiguity in time (Cettolo & Francescato, 2018). In comparison to other commonly used 'alveolar' real-time BbB algorithms (e.g. Auchincloss, Gilbert, & Baule, 1966; Wessel, Stout, Bastanier, & Paul, 1979), the new algorithm has been shown to reduce the fluctuations of the gas exchange data by ~30%, either during moderate-intensity steady-state exercise or during transients (Francescato & Cettolo, 2019).

The different calculation algorithms have usually been compared at rest or when limiting the exercise to the moderate-intensity domain (Auchincloss et al., 1966; Beaver, Lamarra, & Wasserman, 1981; Busso & Robbins, 1997; Capelli, Cautero, & di Prampero, 2001; Cautero, di Prampero, & Capelli, 2003; Grønlund, 1984; Swanson, 1980; Wessel et al., 1979; Wüst, Aliverti, Capelli, & Kayser, 2008); in a limited number of studies, volunteers reached oxygen uptakes as high as ~3.5 l min^{-1} (Gimenez & Busso, 2008; Hughson, Northey, Xing, Dietrich, & Cochrane, 1991; Koga et al., 1989; Wilmore & Costill, 1973). A cycle-ergometer exercise protocol was adopted to evaluate the outcomes of the 'independent breath' algorithm (Francescato & Cettolo, 2019), in agreement with the majority of comparisons among gas exchange calculation algorithms (Beaver et al., 1981; Beaver, Wasserman, & Whipp, 1973; Capelli et al., 2001; Cautero et al., 2003; di Prampero & Lafortuna, 1989; Gimenez & Busso, 2008; Hughson et al., 1991; Koga et al., 1989; Swanson, 1980; Wüst et al., 2008). Limb movements and breathing, however, might not be isolated actions (Stickford & Stickford, 2014). Moreover, during running, the flow sensor (e.g. the turbine of a metabolic unit) might be subjected to variable mechanical stress, in turn affecting the gas exchange values. Accordingly, a thorough picture of the outcomes of different calculation algorithms can be obtained only if a comparison for high-intensity treadmill exercise is also included.

The aim of the present study was the comparison of the gas exchange data obtained by applying different calculation algorithms to data collected from volunteers running on a treadmill, up to high-intensity exercise. We hypothesized that, even during high-speed running, the breath-by-breath gas exchange data yielded by the 'independent breath' algorithm would show less BbB fluctuation compared with the values provided by other commonly used real-time BbB algorithms.

New Findings

- **What is the central question of this study?**
  Breath-by-breath gas exchange analysis during treadmill exercise can be disturbed by different breathing patterns depending on cadence, and the flow sensor might be subjected to variable mechanical stress. It is still unclear whether the outcomes of the gas exchange algorithms can be affected by running at different speeds.
- **What is the main finding and its importance?**
  Practically, the three investigated breath-by-breath algorithms ('Wessel', 'expiration-only' and 'independent breath') provided similar average gas exchange values for steady-state conditions. The 'independent breath' algorithm showed the lowest breath-by-breath fluctuations in the gas exchange data compared with the other investigated algorithms, both at steady state and during incremental exercise.

2 | METHODS

2.1 | Ethical approval

The study conformed to the standards set by the latest revision of the *Declaration of Helsinki*, except for registration in a database, and the experimental procedures were approved by the Institutional Review Board of the German Sport University Cologne (no. 129/2017 issued on 20 September 2017 to J.C. and U.H). After having been thoroughly informed about the experimental protocol, written informed consent was obtained from all subjects before their participation.

2.2 | Participants

Data from 17 individuals (11 males and six females) were analysed. Volunteers were 32.3 ± 8.8 years old (mean ± SD); their stature and body mass were 1.78 ± 0.09 m and 76.0 ± 12.9 kg, respectively. All subjects were experienced in running on a treadmill; all of them trained two to four times per week for a total duration of 6 ± 3 h. The type of training was aimed either for long-distance endurance sports or for predominantly interval-based sports (for more details, see Koschate et al., 2019).

2.3 | Experimental set-up

All participants completed the protocol (Figure 1) on the treadmill (h\p\cosmos pulsar; h\p\cosmos sports & medical GmbH, Nussdorf-Traunstein, Germany). The protocol included 3 min of rest in the standing position (WR_0), followed by 5 min of running at 6.5 km h^{-1} (WR_1), two 5-min-long sequences of pseudo-randomized changes of running velocity (these data were used for the assessment of cardio-respiratory kinetics reported in another paper; Koschate et al., 2019), and 5 min of running at 9.5 km h^{-1} (WR_2). Thereafter, without interruption, volunteers underwent an incremental ramp protocol (WR_{Incr}) to assess peak oxygen uptake. During this period, the speed was first increased automatically by 1 km h^{-1} each minute up to 14 km h^{-1}; then, work intensity was increased by changing the inclination of the treadmill by 1% every 30 s. When the subject was unable to maintain the speed given by the treadmill, the ramp protocol was stopped, and an active recovery phase of 5 min was started, walking at 3.6 km h^{-1}.

Respiratory flow ($\dot{V}$), O_2 and CO_2 fractions (F_{O_2} and F_{CO_2}, respectively) were continuously recorded at the mouth during the trial (CPET Metalyzer 3B, Cortex, Liepzig, Germany) through

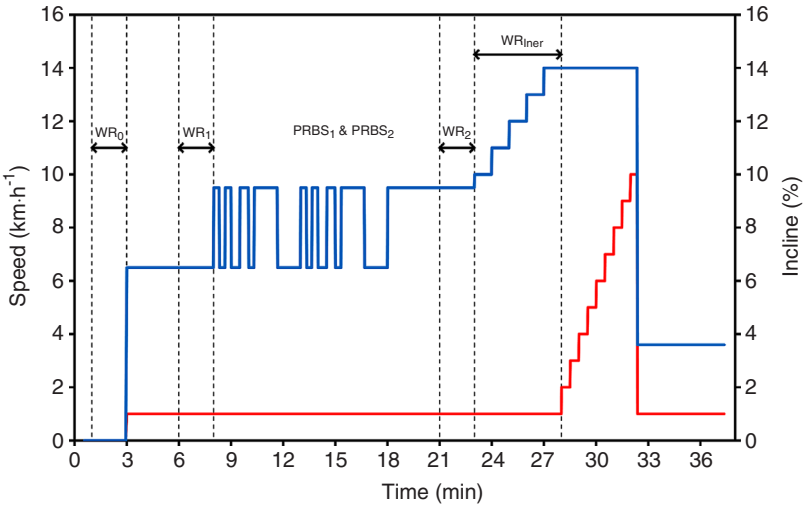

FIGURE 1 Schematic representation of the experimental protocol. Thick blue line illustrates the running speed; thin red line is the incline of the treadmill. Segments limited by arrows represent the time intervals analysed as steady-state conditions (WR_0, WR_1 and WR_2) or as incremental exercise (WR_{Incr})

oronasal silicon masks (deadspace, 88–125 ml; Hans-Rudolf Inc., Shawnee, KS, USA). Gases were sampled through a ~2-m long capillary line inserted in the outer frame of the flow meter and analysed by fast-response electrochemical O_2 and infrared CO_2 sensors embedded in the metabolic cart. The software operating the metabolic cart allowed the recording of gas fractions and flow signal with a sampling frequency of 50 Hz; these signals were saved in text files. The traces of gas fractions and flow were temporally synchronized by the firmware of the metabolic unit, which also converted flow to BTPS conditions. Before each test, following the procedures indicated by the manufacturer, the analysers were calibrated with a gas mixture of known composition [F_{O_2} = 15.0%; F_{CO_2} = 5.0%; N_2 fraction (F_{N_2}) as balance] and ambient air; the flow meter was calibrated by means of a 3 litre syringe (Cortex, Liepzig, Germany).

Timings of the trial, and the speed and inclination of the treadmill, were controlled and automatically recorded by the metabolic unit until the end of the active recovery.

2.4 | Data treatment

For all the volunteers, breath-by-breath oxygen uptake was calculated by means of all the algorithms under investigation, i.e. the 'independent breath' approach (IND), the 'Wessel' approach (WES) and the 'expiration-only' approach (EXP), using computerized procedures specifically developed in C language. The same text file containing the gas fractions and flow traces was used for all the algorithms. As a result, three oxygen uptake time series were obtained for each volunteer ($\dot{V}_{O_2}^{IND}$, $\dot{V}_{O_2}^{WES}$ and $\dot{V}_{O_2}^{EXP}$, respectively). Appropriately substituting the O_2 fraction with the CO_2 fraction and changing the mathematical signs, carbon dioxide output was also calculated.

No data were discarded on all the time series before any of the subsequent analyses.

As previously published (Francescato & Cettolo, 2019), the value of one minus the sum of measured O_2 and CO_2 fractions was assumed to represent the sum of all the gases not exchanged at the alveolar-to-capillary membrane and was labelled F_{N_2}. The respiratory cycles were considered valid only if the inspiratory and/or the expiratory volume was >150 ml; if not, the invalid breath was incorporated with the following one. The calculated data were converted to STPD conditions.

2.5 | The 'independent breath' approach

The main characteristic of the 'independent breath' approach is that the start ($t_{1,j}$) and end ($t_{2,j}$) points of the respiratory cycle are identified on the basis of equal expiratory F_{O_2}/F_{N_2} ratios (Cettolo & Francescato, 2015); in turn, these time points delimit the integration interval for the calculations. The equation used to calculate the O_2 uptake for the j-th breath is as follows:

$$\dot{V}_{O_2 j}^{IND} = \frac{\int_{t_{1,j}}^{t_{2,j}} \dot{V} \times F_{O_2}\,dt - \frac{F_{O_2 j}(t_{1,j})}{F_{N_2 j}(t_{1,j})} \times \int_{t_{1,j}}^{t_{2,j}} \dot{V} \times F_{N_2}\,dt}{t_{2,j} - t_{1,j}} \quad (1)$$

As previously described in detail (Cettolo & Francescato, 2018), the 'independent breath' approach delimits each respiratory cycle without taking into account the end time point of the preceding cycle and/or the start time of the subsequent one.

The following procedure is applied to delimit each respiratory cycle on its own: (i) the minimal end-expiratory F_{O_2}/F_{N_2} ratio is searched for the j-th breath and for the preceding expiration; (ii) the higher of the two F_{O_2}/F_{N_2} values found in step (i) is used as reference ratio (indeed, a reference ratio even slightly lower than the highest one will be missed in the expiration where the highest minimal value was found; this condition will hinder the identification of the start or of the end point of that respiratory cycle); (iii) going backwards from the end of the expiration of the j-th breath, the first time point when the F_{O_2}/F_{N_2} ratio corresponds to the reference ratio [as set in step (ii)] is assumed as the end time point of the respiratory cycle ($t_{2,j}$); and (iv) going backwards from the end of the preceding expiration, the first time point when the F_{O_2}/F_{N_2} ratio corresponds to the reference ratio [as set in step (ii)] is assumed as the starting time point of the respiratory cycle ($t_{1,j}$).

2.6 | The 'Wessel' approach

The concepts underlying the algorithm of Wessel et al. (1979) have been described in detail. The equation to calculate the oxygen uptake for the *j*-th breath can be written as follows:

$$\dot{V}_{O_2 j}^{WES} = \frac{\int_{t_{i,j-1}}^{t_{i,j}} \dot{V} \times F_{O_2} dt - \frac{F_{O_2}(t_{x,j})}{F_{N_2}(t_{x,j})} \times \int_{t_{i,j-1}}^{t_{i,j}} \dot{V} \times F_{N_2} dt}{t_{i,j} - t_{i,j-1}} \quad (2)$$

where F_{O_2} and F_{N_2} are the instantaneous oxygen and 'nitrogen' fractions, as assessed at the mouth; time $t_{i,j}$ corresponds to the time point when the flow changes direction and inspiration starts, and $t_{x,j}$ is the time point corresponding to the end-expiratory gas fraction.

Wessel et al. (1979) derived this equation from that of Auchincloss et al. (1966), assuming that the end-expiratory lung volume was nil.

2.7 | The 'expiration-only' approach

Oxygen uptake during the *j*-th breath can be calculated using information obtained only during expiration and applying the Haldane transformation (Roecker, Prettin, & Sorichter, 2005; Ward, 2018), i.e. using the 'expiration-only' approach ($\dot{V}_{O_2}^{EXP}$). The following equation is applied:

$$\dot{V}_{O_2 j}^{EXP} = \frac{\int_{t_{e,j}}^{t_{i,j}} \dot{V} \times F_{O_2} dt - \frac{F_{O_2}}{F_{N_2}} \times \int_{t_{e,j}}^{t_{i,j}} \dot{V} \times F_{N_2} dt}{t_{i,j} - t_{i,j-1}} \quad (3)$$

where F_{O_2} and F_{N_2} are the instantaneous oxygen and 'nitrogen' fractions, as assessed at the mouth; times $t_{i,j}$ and $t_{e,j}$ correspond to the time points when the flow changes direction and inspiration and expiration start, respectively; and F_{O_2} and F_{N_2} correspond to the inspired ambient fractions and were set to 20.93 and 78.77%, respectively. The adjustment for the dead space of the breathing apparatus (V_{BV}), as proposed by Beaver et al. (1973), is neglected in Equation (3). The following term has to be subtracted from the numerator of Equation (3) to apply the adjustment:

$$[F_{O_2} - F_{O_2}(t_{x,j})] \times V_{BV} \quad (4)$$

2.8 | Data analysis

For all the three O_2 uptake time series ($\dot{V}_{O_2}^{IND}$, $\dot{V}_{O_2}^{WES}$ and $\dot{V}_{O_2}^{EXP}$) of each volunteer, steady-state within-subject average values, and corresponding standard deviations (SD), were calculated over three time periods (Figure 1), i.e. (i) at rest (WR_0; from minute 1:00 to minute 3:00); (ii) during running at 6.5 km h^{-1} (WR_1; from minute 6:00 to minute 8:00); and (iii) during running at 9.5 km h^{-1} (WR_2; from minute 21:00 to minute 23:00).

In addition, for each subject and each algorithm ($n = 17 \times 3$ time series), a linear regression was calculated between the oxygen uptake and the time values, including the data of the first 5 min of the incremental part of the protocol (see WR_{Incr} in Figure 1). The analysis was limited to the first 5 min because: (i) only during this period was the increment in workload linear as a function of time; and (ii) for homogeneity of analysis among volunteers, because a few of them were unable to continue running as soon as the inclination of the treadmill was increased. The classical descriptors of the regression lines (i.e. slope and intercept) and the square root of the arithmetic mean of the squares of the residuals (root mean square; RMS) were calculated for each regression. The intercepts were then calculated for the 23rd minute (i.e. the start of the incremental exercise); the RMS were assumed to be an index of the BbB fluctuations throughout the incremental exercise.

2.9 | Statistical analysis

Statistical analyses were performed using SPSS software (Chicago, IL, USA); results were expressed as means ± SD, and significance level was set to $P < 0.05$.

A multivariate analysis of variance (3×3 MANOVA) with repeated measures on the within-subject factors was used to detect differences among the three investigated algorithms (algorithm effect) and the three different steady-state work rates (work-rate effect). Repeated-measures MANOVA was also used to compare the slopes and intercepts calculated for the regression lines of the incremental exercise, and for the RMS values obtained for the three different $\dot{V}_{O_2}$ time series of the same volunteer (algorithm effect). In either case, Mauchly's test was used to check whether the sphericity assumption appeared to be violated; where Mauchly's test was significant, the Huynh–Feldt ε was used to adjust the degrees of freedom. *Post hoc* simple contrast (against the 'independent breath' algorithm or against the resting condition, as appropriate) was used to detect significant differences inside the within-subject effects.

Given that some of the variables failed to show a normal distribution (according to the Shapiro–Wilk test), non-parametric statistical tests (Friedman two-sided tests) were also performed. All the statistically significant differences observed by applying the MANOVA tests were confirmed.

The magnitude of the differences was also evaluated by calculating the Cohen's *d* effect size (Riemann & Lininger, 2018; Sullivan & Feinn, 2012).

The correlation between variables was assessed by means of the Pearson's correlation coefficient, and the least-squares method was applied to calculate the slopes and intercepts of the regression lines, together with the corresponding widths of the 95% confidence intervals and statistical significance levels against the identity line (i.e. slope = 1 and intercept = 0). In addition, the original Bland and Altman's limits-of-agreement plot with corresponding 95% confidence limits (Bland & Altman, 1986) and the analysis for repeated measures (Bland & Altman, 2007) were used to assess the agreement between the investigated algorithms.

The O_2 uptake values provided by the different algorithms were also evaluated using the trend interchangeability method, which was designed to define the interchangeability of each change of a variable (Fischer et al., 2016). The plug-and-play method provided by Fisher et al. (2016), first classifies each change as uninterpretable or interpretable; among the latter, each case is classified further as

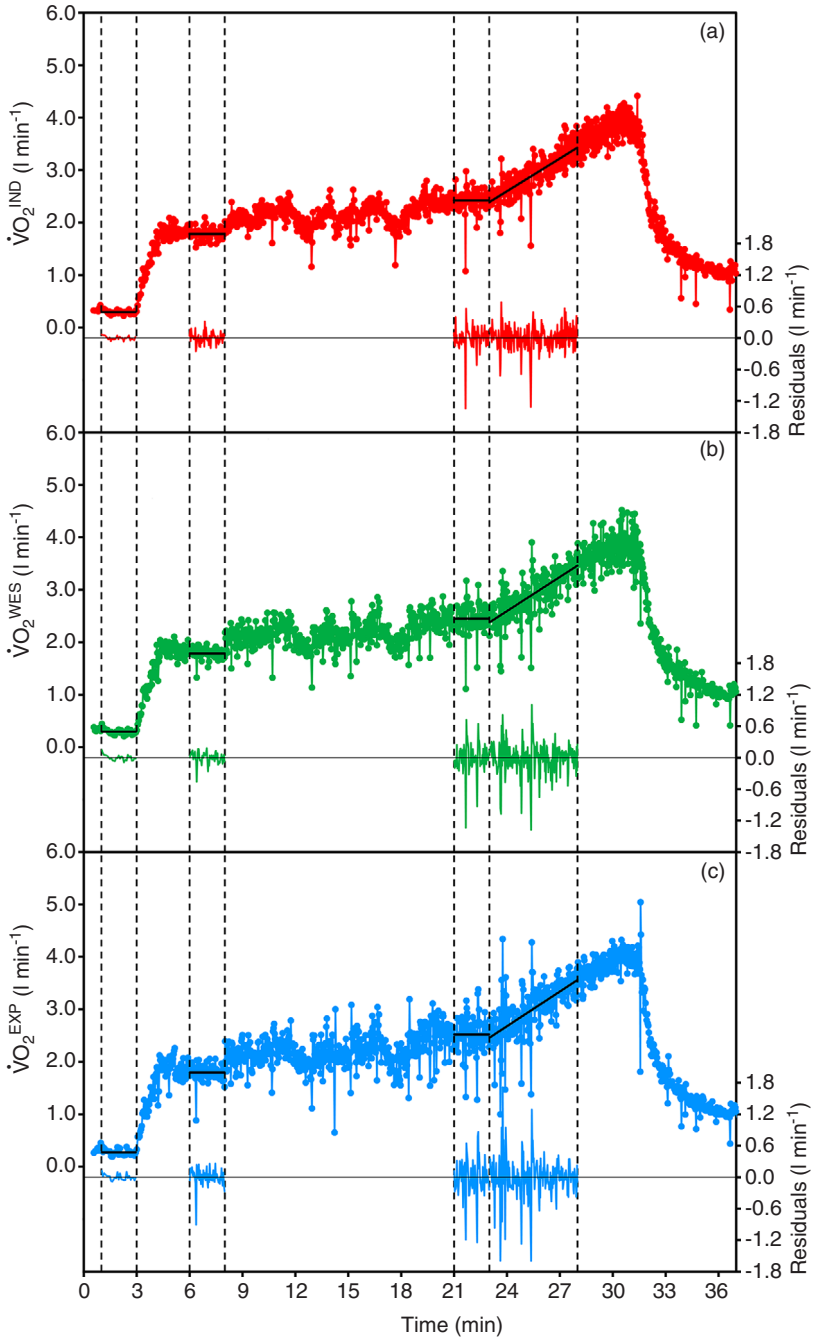

FIGURE 2 Oxygen uptake data obtained for one volunteer applying the 'independent breath' algorithm (a), the 'Wessel' algorithm (b) and the 'expiration-only' algorithm (c); the same original flow and gas fraction traces were used for all the algorithms. The average values for the steady-state conditions (WR_0, WR_1 and WR_2) and the 'best-fit' linear regression line for the incremental exercise (WR_{Incr}) are illustrated for all the algorithms as continuous lines; corresponding residuals are plotted below (right axis)

interchangeable, in the grey zone or non-interchangeable, on the basis of the repeatability coefficient set for the reference method. The trend interchangeability rate is then calculated as the ratio of the number of interchangeable changes and the total number of interpretable changes. A range of reasonable repeatability coefficients was explored.

3 | RESULTS

Figure 2 illustrates the O_2 uptake values obtained for one volunteer by applying the three algorithms under investigation. The panels show the same behaviour for the O_2 uptake values as a function of time, although different BbB fluctuations can be noted.

3.1 | Analysis of the steady-state work rates

The between-subject averages of the within-subject mean oxygen uptake values obtained for the three steady-state work rates (i.e. rest and running at 6.5 and at 9.5 km h^{-1}) using the three algorithms under investigation are summarized in Table 1, together with the corresponding average standard deviations and Cohen's *d* effect sizes.

The mean oxygen uptakes yielded by the 'independent breath', the 'Wessel' and the 'expiration-only' algorithms for the three steady-state

TABLE 1 Steady-state O_2 uptake values obtained using the time series yielded by the three algorithms under investigation

	Time series				
	'Independent breath'	'Wessel'		'Expiration-only'	
Conditions	(l min^{-1})	(l min^{-1})	ES	(l min^{-1})	ES
Rest (WR_0)					
Mean	0.333 ± 0.070	0.334 ± 0.069	0.01	0.338 ± 0.078	0.06
SD	0.065 ± 0.033	0.073 ± 0.035	0.24	0.083 ± 0.039**	0.55
Running at 6.5 km h^{-1} (WR_1)					
Mean	1.944 ± 0.348	1.954 ± 0.352*	0.03	2.035 ± 0.354***	0.26
SD	0.154 ± 0.065	0.231 ± 0.087***	1.18	0.254 ± 0.118***	1.55
Running at 9.5 km h^{-1} (WR_2)					
Mean	2.612 ± 0.536	2.628 ± 0.549*	0.03	2.770 ± 0.579***	0.30
SD	0.208 ± 0.062	0.257 ± 0.063***	0.79	0.272 ± 0.098**	1.03

Values are the between-subjects means ± SD of the within-subject averages and standard deviations. $n = 17$ overall. Values significantly different from $\dot{V}_{O_2}^{IND}$ values (Student's paired t test for each condition) are indicated as follows: $^{*}P < 0.05$, $^{**}P < 0.01$ and $^{***}P < 0.001$. Abbreviation: ES, Cohen's d effect sizes for the comparison between the values obtained for $\dot{V}_{O_2}^{WES}$ or $\dot{V}_{O_2}^{EXP}$ *versus* $\dot{V}_{O_2}^{IND}$.

work rates were significantly different (algorithm effect, $F = 23.0$, $P < 0.001$); *post hoc* contrasts revealed that the 'independent breath' approach yielded significantly lower oxygen uptake values compared with the other two algorithms ($F > 14.89$, $P < 0.001$ for both). In turn, the three steady-state work rates showed significantly different average values (work-rate effect, $F = 329$, $P < 0.001$); in comparison to rest, the running phases (WR_1 and WR_2) showed increasingly higher values with increasing speed ($F > 341.7$, $P < 0.001$).

The average $\dot{V}_{O_2}^{IND}$ values are plotted against the corresponding average $\dot{V}_{O_2}^{WES}$ or $\dot{V}_{O_2}^{EXP}$ values in Figure 3a,b; the data for all the steady-state work rates (i.e. WR_0, WR_1 and WR_2) are illustrated. It can be observed that all the $\dot{V}_{O_2}^{IND}$ values were within 5% of the identity line with the $\dot{V}_{O_2}^{WES}$ values, whereas in 29 of 51 cases the $\dot{V}_{O_2}^{IND}$ values were within 5% of the identity line with the $\dot{V}_{O_2}^{EXP}$ values. The corresponding original Bland–Altman plots are shown in Figure 3c,d; the mean difference (i.e. the bias) between the $\dot{V}_{O_2}^{WES}$ and the $\dot{V}_{O_2}^{IND}$ values was |9 ml min^{-1}|, whereas it amounted to |84 ml min^{-1}| when the difference between $\dot{V}_{O_2}^{EXP}$ and $\dot{V}_{O_2}^{IND}$ values was considered. Accounting for the repeated measurements, the radius of the 95% interval of agreement of the differences between the 'independent breath' and the 'Wessel' algorithms was ± 50 ml min^{-1}; the corresponding value with the 'expiration-only' values was more than fourfold greater (±205 ml min^{-1}).

The analysis on the within-subject standard deviations calculated for the same three steady-state time periods as above (Table 1) showed that they were significantly different among the time series provided by the three algorithms under comparison (algorithm effect, $F = 45.3$, $P < 0.001$). *Post hoc* contrasts showed that the smallest standard deviations were those obtained for $\dot{V}_{O_2}^{IND}$ in comparison to the other two time series (*post hoc* contrast, $F > 47.23$, $P < 0.001$). A significant difference was observed among the three steady states of the investigated work rates (work-rate effect, $F = 33.8$, $P < 0.001$), with the running phases showing significantly greater standard deviations compared with the resting condition (*post hoc* contrast, $F > 43.24$, $P < 0.001$). Figure 4 illustrates the standard deviations obtained for the BbB data provided by the 'independent breath' algorithm as a function of the corresponding values obtained for the $\dot{V}_{O_2}^{WES}$ and the $\dot{V}_{O_2}^{EXP}$ time series; data for all volunteers and all steady-state work rates are illustrated. The correlation was statistically significant in both cases ($R > 0.850$, $P < 0.001$, $n = 51$), although both regression lines were far from the identity line. Indeed, the slope of the linear regression between the paired data amounted to 0.70 and 0.55 for the $\dot{V}_{O_2}^{WES}$ and the $\dot{V}_{O_2}^{EXP}$ time series, respectively; these values were significantly lower than one in both cases ($t > 6.35$, $P < 0.001$), with the intercept being significantly different from zero only for the $\dot{V}_{O_2}^{EXP}$ time series ($t = 2.60$, $P < 0.05$).

Figure 5 illustrates, classified according to the trend interchangeability method, the percentage cases of the differences between the mean values of $\dot{V}_{O_2}^{IND}$ and $\dot{V}_{O_2}^{WES}$ (Figure 5a) or $\dot{V}_{O_2}^{EXP}$ (Figure 5b) as a function of the repeatability coefficient (in the range 0–25%). The behaviours of the trend interchangeability rate of the IND algorithm with respect to the two reference algorithms (EXP and WES) are superimposed in Figure 5; in either case, the trend interchangeability rate was >95% for a repeatability coefficient >12%.

Analogous results were obtained for CO_2 output and are summarized in Table 2.

3.2 | Incremental exercise

The averages of the linear regression parameters of the incremental exercises, the corresponding RMS values (i.e. the square root of the average of the squares of the vertical distances between data points and the regression line) and the appropriate Cohen's d effect sizes are reported in Table 3. Results obtained using the O_2 uptake time series provided by the three algorithms under investigation ($\dot{V}_{O_2}^{IND}$, $\dot{V}_{O_2}^{WES}$ and $\dot{V}_{O_2}^{EXP}$) are reported.

The slopes of the regression lines calculated using the $\dot{V}_{O_2}$ yielded by the three algorithms were not statistically different (algorithm

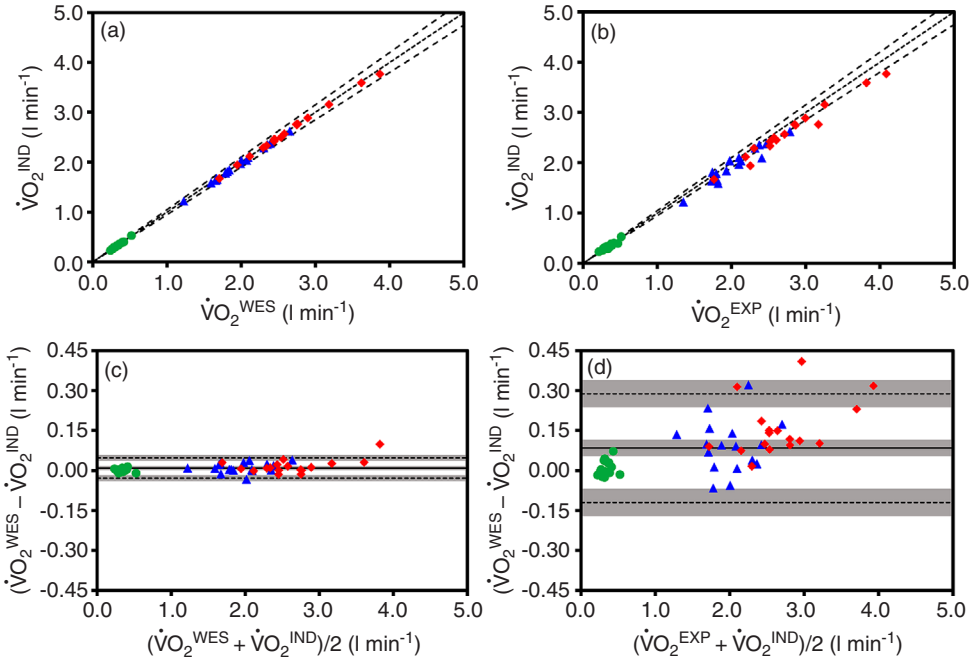

FIGURE 3 Average steady-state O_2 uptakes of the three steady-state conditions as obtained, for all the 17 volunteers, from the $\dot{V}_{O_2}^{IND}$ data are plotted against the corresponding values obtained for the 'Wessel' (a) and the 'expiration-only' (b) algorithms. Dotted lines are 5% change from the identity line. (c,d) The corresponding original Bland–Altman plots are illustrated. Continuous lines represent the bias. Dotted lines are the 95% limits of agreement. Shaded areas indicate the corresponding 95% confidence intervals. The three steady-state work rates are illustrated with different symbols: circles, rest (WR_0); triangles, running at 6.5 km h^{-1} (WR_1); and diamonds, running at 9.5 km h^{-1} (WR_2)

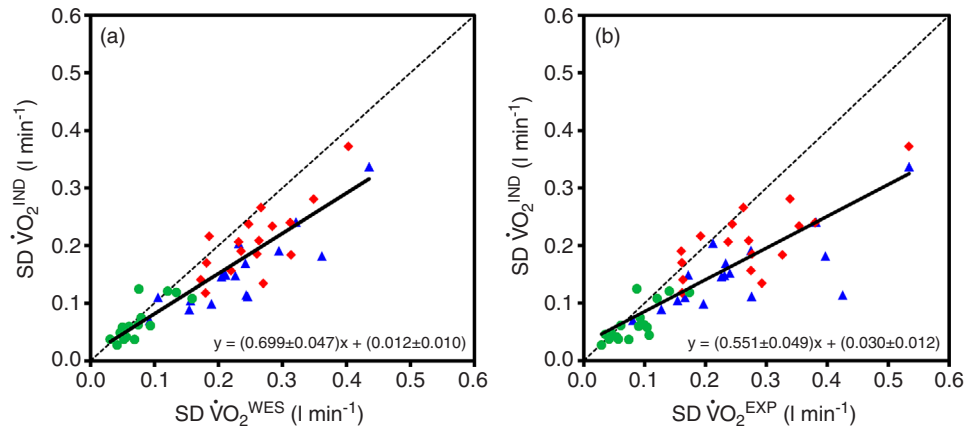

FIGURE 4 Standard deviations (SDs) calculated for the O_2 uptakes provided by the 'independent breath' algorithm are plotted against the corresponding values obtained for the 'Wessel' (a) and the 'expiration-only' (b) algorithms. Continuous lines are the corresponding regression lines. Dotted lines are the identity lines. The three steady-state work rates are illustrated with different symbols: circles, rest (WR_0); triangles, running at 6.5 km h^{-1} (WR_1); and diamonds, running at 9.5 km h^{-1} (WR_2)

effect, $F = 0.207$, P = n.s.), with the grand average of all slopes amounting to 0.171 ± 0.054 l min^{-2}. The corresponding intercepts were significantly different among the three algorithms (algorithm effect, $F = 32.2$, $P < 0.001$), being greater for $\dot{V}_{O_2}^{EXP}$ compared with those obtained for $\dot{V}_{O_2}^{WES}$ or $\dot{V}_{O_2}^{IND}$ (Table 3; *post hoc* contrast, $F = 33.0$, $P < 0.001$).

The RMSs were significantly different among the three algorithms (algorithm effect, $F = 5.14$, $P < 0.05$), with the $\dot{V}_{O_2}^{IND}$ showing significantly lower values compared with both other algorithms (*post hoc* contrast, $F > 4.78$, $P < 0.05$). Figure 6 illustrates, for all volunteers, the RMSs obtained for the data provided by the 'independent breath' algorithm as a function of the corresponding values obtained for the $\dot{V}_{O_2}^{WES}$ or the $\dot{V}_{O_2}^{EXP}$ time series. In both cases, the correlation between the two variables was statistically significant ($r > 0.809$, $P < 0.001$, $n = 17$). The intercepts of the two regression lines were not significantly different from zero ($t < 1.17$, P = n.s.), whereas the slopes amounted to 0.84 and 0.70, respectively, being significantly lower than one ($t > 2.32$, $P < 0.05$) only for the RMS of the $\dot{V}_{O_2}^{EXP}$ time series.

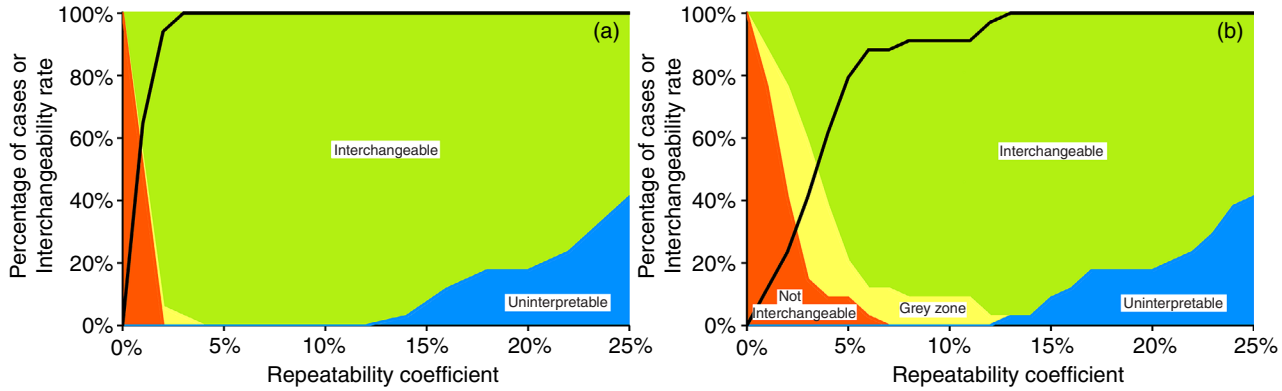

FIGURE 5 Percentage cases of the differences between the mean oxygen uptake values obtained for the 'independent breath' and the 'Wessel' algorithms (a) or the 'expiration-only' (b) algorithm as a function of the repeatability coefficient of the latter, classified according to the trend interchangeability method. Thick black lines are the trend interchangeability rate of the IND algorithm with respect to the two reference algorithms (EXP or WES). Blue area indicates uninterpretable cases; orange area indicates non-interchangeable cases; yellow area indicates grey zone cases; and green area indicates interchangeable cases (see Methods)

TABLE 2 Steady-state CO_2 output values obtained using the time series yielded by the three algorithms under investigation

	Time series				
	'Independent breath'	'Wessel'		'Expiration-only'	
Conditions	(l min^{-1})	(l min^{-1})	ES	(l min^{-1})	ES
Rest (WR_0)					
Mean	0.280 ± 0.059	0.280 ± 0.060	0.01	0.294 ± 0.073*	0.23
SD	0.062 ± 0.029	0.063 ± 0.029	0.04	0.072 ± 0.033*	0.33
Running at 6.5 km h^{-1} (WR_1)					
Mean	1.643 ± 0.339	1.643 ± 0.341	0.01	1.775 ± 0.360***	0.39
SD	0.159 ± 0.054	0.198 ± 0.072***	0.74	0.223 ± 0.096***	1.20
Running at 9.5 km h^{-1} (WR_2)					
Mean	2.362 ± 0.591	2.372 ± 0.599*	0.02	2.624 ± 0.663***	0.44
SD	0.207 ± 0.057	0.238 ± 0.065**	0.55	0.254 ± 0.094**	0.83

Values are the between-subjects means ± SD of the within-subject averages and standard deviations. $n = 17$ overall. Values significantly different from $\dot{V}_{CO_2}^{IND}$ values (Student's paired t test for each condition) are indicated as follows: $^{*}P < 0.05$, $^{**}P < 0.01$ and $^{***}P < 0.001$. Abbreviation: ES, Cohen's d effect sizes for the comparison between the values obtained for $\dot{V}_{CO_2}^{WES}$ or $\dot{V}_{CO_2}^{EXP}$ *versus* $\dot{V}_{CO_2}^{IND}$.

TABLE 3 Average slope, intercept and root mean square values obtained by linear regression during the incremental exercise (WR_{Incr}) using the $\dot{V}_{O_2}^{IND}$, $\dot{V}_{O_2}^{WES}$ or $\dot{V}_{O_2}^{EXP}$ data against time ($n = 17$ overall)

	Time series				
	'Independent breath'	'Wessel'		'Expiration-only'	
Parameter			ES		ES
Slope (l min^{-2})	0.170 ± 0.055	0.172 ± 0.054	0.03	0.173 ± 0.056	0.04
Intercept (l min^{-1})	2.602 ± 0.539	2.609 ± 0.552	0.01	2.747 ± 0.581***	0.27
Residual sum of squares (l min^{-1})	0.237 ± 0.087	0.259 ± 0.091*	0.26	0.276 ± 0.101*	0.45

The intercept values are those calculated for the start of incremental exercise (i.e. minute 23). Values significantly different from $\dot{V}_{O_2}^{IND}$ values (Student's paired t test for each condition) are indicated as follows: $^{*}P < 0.05$, $^{**}P < 0.01$ and $^{***}P < 0.001$. Abbreviation: ES, Cohen's d effect sizes for the comparison between the values obtained for $\dot{V}_{O_2}^{WES}$ or $\dot{V}_{O_2}^{EXP}$ *versus* $\dot{V}_{O_2}^{IND}$.

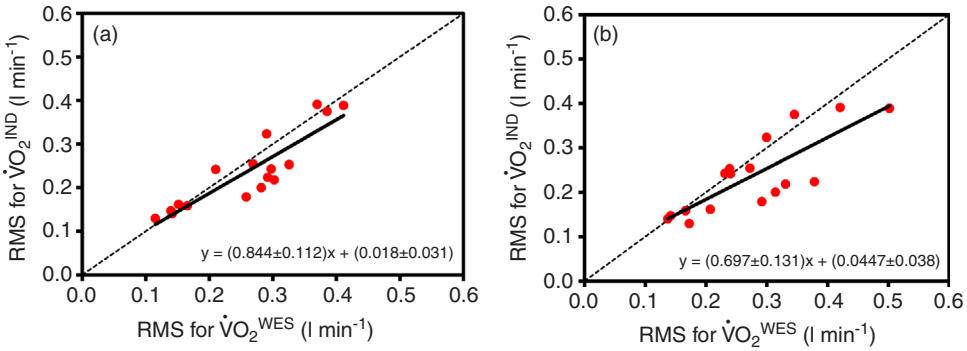

FIGURE 6 Individual root mean square (RMS) values obtained from the linear regression of the O_2 uptake time series *versus* time for the incremental exercise (WR_{Incr}). The RMS values obtained with the 'independent breath' algorithm are plotted as a function of the corresponding values obtained using the 'Wessel' algorithm (a) or the 'expiration-only' algorithm (b). Data of all the 17 volunteers are plotted. Continuous lines are the corresponding regression lines. Dotted lines are the identity lines

4 | DISCUSSION

The present paper is the first comparing the O_2 uptake values obtained from volunteers running on a treadmill up to high speed, calculated with different BbB gas exchange algorithms. Statistically significant differences were observed for the average values and for the indexes of BbB fluctuations.

4.1 | Steady-state work rates

In steady-state conditions, the average $\dot{V}_{O_2}$ values obtained with the IND algorithm were lower compared with the corresponding values yielded by both the WES and EXP algorithms.

The difference observed between the average $\dot{V}_{O_2}^{WES}$ and $\dot{V}_{O_2}^{IND}$ values might be explained by the fact that, for its calculations, the IND algorithm uses the highest value between the minimal end-expiratory F_{O_2}/F_{N_2} ratios identified in two subsequent expirations, thus resulting in lower $\dot{V}_{O_2}$ values. Although statistically significant, from a practical point of view the difference was negligible. Indeed, the effect size value amounted at most to 0.03 for the three investigated work rates, being lower than the threshold value for a small difference (Riemann & Lininger, 2018; Sullivan & Feinn, 2012); moreover, all the values were within 5% of the identity line.

During the running phases, the average $\dot{V}_{O_2}^{EXP}$ values were significantly higher than the corresponding $\dot{V}_{O_2}^{IND}$ values, albeit the effect size was still small. The EXP algorithm was applied while neglecting the possible correction for the dead space of the breathing apparatus (Ward, 2018). This correction was suggested by Beaver et al. (1973) on the basis of the reasoning that at the beginning of inspiration, inspired air is not room air but is end-tidal expired air from the previous breath, because the dead space of the breathing apparatus contains expired air. The correction was proposed because the information was collected using breathing valves and during the expiration phases only; it is likely to be dependent on breathing frequency (Porszasz, Stringer, & Casaburi, 2007) and/or on tidal volume (Bradley & Younes, 1980). Currently, this adjustment is under debate, in particular given that contemporary metabolic units mainly use flow sensors that operate bi-directionally (Ward, 2018). To test the effect of the dead space correction, the gas exchange values of the present investigation were recalculated with the EXP algorithm, introducing an arbitrary volume of 99 ml for the dead space of the breathing apparatus. Overall, the newly obtained $\dot{V}_{O_2}^{EXP}$ values were reduced; they became similar to the values yielded by the IND algorithm at the highest running speed (i.e. 2.576 ± 0.578 *versus* 2.612 ± 0.536 l min^{-1}), but at rest they became significantly lower than the values obtained with the IND algorithm, with a large effect size (i.e. 0.277 ± 0.070 *versus* 0.333 ± 0.070 l min^{-1}; effect size = 0.81). These results suggest that the fixed dead-space volume correction applied was not adequate to remove all the differences between the O_2 uptakes obtained using the IND and EXP algorithms in all the investigated conditions.

The BbB fluctuations of the data obtained with the IND algorithm, evaluated through the standard deviations, was always significantly lower compared with the other two algorithms under investigation. The slopes of the regression lines between the paired values (0.70 and 0.55 for the values obtained with the WES and EXP algorithms, respectively) were significantly lower than one in both cases (Figure 4). These slopes were similar to the analogous slopes obtained at lower steady-state exercise intensity (Francescato & Cettolo, 2019). The difference in the standard deviations increased from a small effect size at rest (0.2 < effect size < 0.6) to a definitely large difference (effect size >0.8) during running, suggesting an effect linked to the exercise intensity.

It is noteworthy that, in contrast to the 'expiration-only' algorithm, the 'Wessel' and the 'independent breath' algorithms were both theoretically designed to account for the changes in lung gas stores. This might explain, at least in part, the lower standard deviations of the latter two algorithms compared with the 'expiration-only' one.

The discussion here above suggests that knowledge of the algorithm used for the calculation of the gas exchange data might be of relevance for an appropriate evaluation of the information collected, even when the measurements are performed at steady state and not only when the kinetics of O_2 uptake during transients are being investigated (Golja, Cettolo, & Francescato, 2018).

Although Bland–Altman analysis is of widespread use, it does not provide objective information concerning the interchangeability of the methods/devices under comparison. To overcome this problem, the trend interchangeability method has recently been proposed (Fischer et al., 2016). For the first time, this method was applied to the comparison of $\dot{V}_{O_2}$ data obtained by different breath-by-breath gas exchange algorithms. Figure 5 shows that the areas of the 'not interchangeable' and of the 'grey zone' cases are wider in the IND *versus* EXP comparison, in comparison to those obtained in the IND *versus* WES comparison. This explains why, in the IND *versus* WES comparison, the trend interchangeability rate (the black lines in Figure 5) reaches 100% even for small repeatability coefficients. The repeatability coefficients calculated according to Bland and Altman (1986) amounted to 12, 16 and 17% for the O_2 uptakes yielded by IND, WES and EXP algorithms, respectively. Consequently, according to the trend interchangeability method, the average $\dot{V}_{O_2}$ values yielded by the three algorithms under investigation for the analysed steady-state conditions are completely interchangeable.

4.2 | Incremental exercise

The intercept of the regression lines of $\dot{V}_{O_2}$ *versus* time, calculated for the time at the start of the incremental exercise (i.e. minute 23), reflected, for all the algorithms, the values obtained for the steady-state running period at 9.5 km h^{-1}, maintaining the observed differences among the algorithms. The increases of $\dot{V}_{O_2}$ per minute during the incremental phase of the protocol (namely, the slopes of the regression lines) were not significantly different among the three investigated algorithms. It can thus be inferred that the differences observed among the algorithms at the highest steady-state running speed will also be reflected at the maximal exercise intensity reached by the subjects, probably maintaining a similar small effect size.

The RMSs, taken as index of the BbB fluctuations of the $\dot{V}_{O_2}$ values during the incremental phase of the protocol, were significantly lower for the data obtained with the IND algorithm compared with the other two algorithms under investigation. Nevertheless, the slope resulting from the regression line between paired RMSs was significantly lower than one (i.e. 0.70) only for the values obtained with the EXP algorithm (Figure 6). These results show that, even during high-speed running, the O_2 uptake values obtained with the IND algorithm show less BbB fluctuation than those yielded by the other two algorithms under investigation.

4.3 | Impact of the 'independent breath' approach on the respiratory variables

The calculations of gas exchange by means of all the algorithms under investigation are based on the same raw traces of gas fractions and flow, and, consequently, the respiratory variables directly obtained from the raw traces (e.g. end-tidal O_2 and CO_2 fractions) remain the same, independent of the definition of the respiratory cycle used.

The alternative definition of the respiratory cycle, used in the 'independent breath' approach, is different from the classical one because the start and end points of the respiratory cycle are identified by the F_{O_2}/F_{N_2} ratio (or F_{CO_2}/F_{N_2} ratio) and allow the partial superposition or disjunction in time of subsequent cycles (Cettolo & Francescato, 2018). This alternative definition of the respiratory cycle was introduced to account for the changes in lung gas stores, with the aim of estimating the O_2 uptake (or CO_2 output) at the alveolar-to-capillary membrane. We believe that the gas exchange values obtained with the 'independent breath' algorithm, being correct for the changes in lung gas stores, might provide prognostic and diagnostic information in addition to that yielded by the 'classical' algorithms.

There is no rationale for the adoption of the alternative view of the respiratory cycle for the calculation of other respiratory variables dependent on breath duration (such as ventilation), because for these variables there are no lung gas stores to account for. In addition, practically equal mean values (and standard deviations) were obtained for the respiratory frequency and tidal volume calculated from our experimental traces using the two definitions of the respiratory cycle (data not shown).

Further work is needed to depict the effects of the alternative definition of the respiratory cycle on the relationships among respiratory variables (as investigated in cardiorespiratory exercise testing) and on their fluctuations in clinical conditions (e.g. in patients suffering from breathing pattern disorders or in patients with heart failure showing exercise oscillatory ventilation).

4.4 | Strengths and limitations

At variance with previous similar studies, almost all of which have used cycle-ergometer exercise (Beaver et al., 1981; Capelli et al., 2001; Cettolo & Francescato, 2015; Swanson, 1980), in the present work the gas exchange calculation algorithms under investigation were applied on traces collected from subjects running at different speeds, up to very intense exercise.

For the first time, a recently proposed method (Fischer et al., 2016), so far used mainly for the comparison of devices to assess cardiac output, has been applied to compare the average gas exchange data. The criteria for interpretation of the results of this method, and its limitations and/or potentiality, however, are yet to be elucidated fully.

The analysis was limited to the steady-state time periods and to the first 5 min of the incremental exercise, neglecting a large portion of the acquired data. Nevertheless, the BbB fluctuations during the pseudo-random binary sequence periods would be difficult to analyse, owing to the frequently changing work rates and the particular data treatment applied to obtain useful physiological information from this exercise protocol (Koschate et al., 2019). During the incremental exercise, only the first 5 min were completed by all the volunteers, with the same linear increase in work rate according to time, thus allowing for a homogeneous analysis across subjects. Any analysis after this period would be linked too greatly to subjective and arbitrary evaluation (Poole & Jones, 2017), in the absence of any commonly accepted procedure to account for the BbB fluctuations in the gas exchange values.

4.5 | Conclusions

The present work confirmed and extended the results obtained previously at lower exercise intensities during cycle ergometry. Indeed, the three algorithms under investigation provided practically overlapping average gas exchange values, although the difference in the values obtained using the EXP algorithm was dependent on the exercise intensity and on the adjustment (or not) for the dead space.

Compared with the other investigated calculation algorithms, the IND algorithm was the one yielding data with the lowest BbB fluctuations, both at steady state and during the incremental exercise.

Given that differences were observed among the investigated algorithms, we make the following suggestions: (i) the algorithms should also be tested for high exercise intensities; and (ii) in experimental papers, it would be appropriate always to cite the BbB gas exchange algorithm used.

ACKNOWLEDGEMENTS

We would like to thank Laura Gerlich and Veronika Wirtz for their support during the measurements.

COMPETING INTERESTS

None declared.

AUTHOR CONTRIBUTIONS

U.H. and M.P.F. conceived the work. J.K. acquired the data. V.C. and M.P.F. analysed and interpreted the data and wrote the draft of the paper. All authors critically revised the paper and approved the final version. All the authors agree to be accountable for all aspects of the work in ensuring that questions related to the accuracy or integrity of any part of the work are appropriately investigated and resolved. All persons designated as authors qualify for authorship, and all those who qualify for authorship are listed.

ORCID

Valentina Cettolo https://orcid.org/0000-0003-0577-1317
Maria Pia Francescato https://orcid.org/0000-0002-7892-863X

REFERENCES

Auchincloss, J. H. Jr, Gilbert, R., & Baule, G. H. (1966). Effect of ventilation on oxygen transfer during early exercise. *Journal of Applied Physiology*, *21*, 810–818.

Beaver, W. L., Lamarra, N., & Wasserman, K. (1981). Breath-by-breath measurement of true alveolar gas exchange. *Journal of Applied physiology: Respiratory, Environmental and Exercise Physiology*, *51*, 1662–1675.

Beaver, W. L., Wasserman, K., & Whipp, B. J. (1973). On-line computer analysis and breath-by-breath graphical display of exercise function tests. *Journal of Applied Physiology*, *34*, 128–132.

Bland, J. M., & Altman, D. G. (1986). Statistical methods for assessing agreement between two methods of clinical measurement. *Lancet*, *1*(8476), 307–310.

Bland, J. M., & Altman, D. G. (2007). Agreement between methods of measurement with multiple observations per individual. *Journal of Biopharmaceutical Statistics*, *17*, 571–582.

Bradley, P., & Younes, M. (1980). Relation between respiratory valve dead space and tidal volume. *Journal of Applied physiology: Respiratory, Environmental and Exercise Physiology*, *49*, 528–532.

Busso, T., & Robbins, P. A. (1997). Evaluation of estimates of alveolar gas exchange by using a tidally ventilated nonhomogenous lung model. *Journal of Applied Physiology*, *82*, 1963–1971.

Capelli, C., Cautero, M., & di Prampero, P. E. (2001). New perspectives in breath-by-breath determination of alveolar gas exchange in humans. *Pflugers Archiv: European Journal of Physiology*, *441*, 566–577.

Cautero, M., di Prampero, P. E., & Capelli, C. (2003). New acquisitions in the assessment of breath-by-breath alveolar gas transfer in humans. *European Journal of Applied Physiology*, *90*, 231–241.

Cettolo, V., & Francescato, M. P. (2015). Assessment of breath-by-breath alveolar gas exchange: An alternative view of the respiratory cycle. *European Journal of Applied Physiology*, *115*, 1897–1904.

Cettolo, V., & Francescato, M. P. (2018). Assessing breath-by-breath alveolar gas exchange: Is the contiguity in time of breaths mandatory? *European Journal of Applied Physiology*, *118*, 1119–1130.

di Prampero, P. E., & Lafortuna, C. L. (1989). Breath-by-breath estimate of alveolar gas transfer variability in man at rest and during exercise. *The Journal of Physiology*, *415*, 459–475.

Fischer, M.-O., Diouf, M., Wilde, R. B. P., Dupont, H., Hanouz, J.-L., & Lorne, E. (2016). Evaluation of cardiac output by 5 arterial pulse contour techniques using trend interchangeability method. *Medicine*, *95*, e3530.

Francescato, M. P., & Cettolo, V. (2019). The "independent breath" algorithm: Assessment of oxygen uptake during exercise. *European Journal of Applied Physiology*, *119*, 495–508.

Gimenez, P., & Busso, T. (2008). Implications of breath-by-breath oxygen uptake determination on kinetics assessment during exercise. *Respiratory Physiology & Neurobiology*, *162*, 238–241.

Golja, P., Cettolo, V., & Francescato, M. P. (2018). Calculation algorithms for breath-by-breath alveolar gas exchange: The unknowns! *European Journal of Applied Physiology*, *118*, 1869–1876.

Grønlund, J. (1984). A new method for breath-to-breath determination of oxygen flux across the alveolar membrane. *European Journal of Applied Physiology and Occupational Physiology*, *52*, 167–172.

Hughson, R. L., Northey, D. R., Xing, H. C., Dietrich, B. H., & Cochrane, J. E. (1991). Alignment of ventilation and gas fraction for breath-by-breath respiratory gas exchange calculations in exercise. *Computers and Biomedical Research*, *24*, 118–128.

Koga, S., Tsushima, S., Uemura, T., Sakurai, T., Takahashi, T., Fukuba, Y., & Ikegami, H. (1989). Breath-by-breath differences between exercise gas exchange kinetics measured at the mouth and those estimated at the alveolar level. *Japanese Journal of Physical Fitness and Sports Medicine*, *38*, 151–164.

Koschate, J., Gerlich, L., Wirtz, V., Thieschäfer, L., Drescher, U., & Hoffmann, U. (2019). Cardiorespiratory kinetics: Comparisons between athletes with different training habits. *European Journal of Applied Physiology*, *119*, 1875–1883.

Poole, D. C., & Jones, A. M. (2017). Measurement of the maximum oxygen uptake $\dot{V}O_{2max}$: $\dot{V}O_{2peak}$ is no longer acceptable. *Journal of Applied Physiology*, *122*, 997–1002.

Porszasz, J., Stringer, W., & Casaburi, R. (2007). Equipment, measurements and quality control in clinical exercise testing. In S. Ward & P. Palange (Eds.), *Clinical exercise testing. European respiratory monograph* (Vol. 40, pp. 108–128). Sheffield: European Respiratory Society Journals.

Riemann, B. L., & Lininger, M. R. (2018). Principles of statistics: What the sports medicine professional needs to know. *Clinics in Sports Medicine*, *37*, 375–386.

Roecker, K., Prettin, S., & Sorichter, S. (2005). Gas exchange measurements with high temporal resolution: The breath-by-breath approach. *International Journal of Sports Medicine*, *26*(Suppl 1), S11–S18.

Stickford, A. S. L., & Stickford, J. L. (2014). Ventilation and locomotion in humans: Mechanisms, implications, and perturbations to the coupling of these two rhythms. *Springer Science Reviews*, *2*, 95–118.

Sullivan, G. M., & Feinn, R. (2012). Using effect size—or why the *P* value is not enough. *Journal of Graduate Medical Education*, *4*, 279–282.

Swanson, G. (1980). Breath-to breath considerations for gas exchange kinetics. In P. Cerretelli & B. J. Whipp (Eds.), *Exercise bioenergetics and gas exchange* (pp. 211–222). Amsterdam: Elsevier/North Holland.

Ward, S. A. (2018). Open-circuit respirometry: Real-time, laboratory-based systems. *European Journal of Applied Physiology*, *118*, 875–898.

Wessel, H., Stout, R., Bastanier, C., & Paul, M. (1979). Breath-by-breath variation of FRC: Effect on VO_2 and VCO_2 measured at the mouth. *Journal of Applied Physiology: Respiratory, Environmental and Exercise Physiology*, *46*, 1122–1126.

Wilmore, J. H., & Costill, D. L. (1973). Adequacy of the Haldane transformation in the computation of exercise VO_2 in man. *Journal of Applied Physiology*, *35*, 85–89.

Wüst, R. C. I., Aliverti, A., Capelli, C., & Kayser, B. (2008). Breath-by-breath changes of lung oxygen stores at rest and during exercise in humans. *Respiratory Physiology & Neurobiology*, *164*, 291–299.

SUPPORTING INFORMATION

Additional supporting information may be found online in the Supporting Information section at the end of the article.

How to cite this article: Koschate J, Cettolo V, Hoffmann U, Francescato MP. Breath-by-breath oxygen uptake during running: Effects of different calculation algorithms. *Experimental Physiology*. 2019;104:1829–1840. https://doi.org/10.1113/EP087916